Dynamically Reentrant Skyrmion Phase in Oscillating Magnetic Fields

Accepted for publication in Physical Review Letters

Dynamically Re-entrant Skyrmion Phase in Oscillating Magnetic Fields

Z. Demir Vatansever,[1,*] E. Vatansever,[1,†] A. Vasilopoulos,[2,‡] N. G. Fytas,[2,§] and A. Berger[3,¶]

[1]*Department of Physics, Dokuz Eylül University, TR-35160, Izmir-Turkey*
[2]*School of Mathematics, Statistics and Actuarial Science, University of Essex, Colchester CO4 3SQ, United Kingdom*
[3]*CIC nanoGUNE BRTA, E-20018 Donostia-San Sebastian, Spain*

(Dated: February 2, 2026)

We address a central open question in driven topological matter by investigating the nonequilibrium response of a two-dimensional magnet with Dzyaloshinskii–Moriya interactions subjected to a periodically oscillating magnetic field. Using extensive Monte Carlo simulations, we uncover a dynamically re-entrant skyrmion phase that emerges within a finite window of field amplitudes and bias fields, sandwiched between the conventional skyrmion and polarized ferromagnetic phases. This phase has no equilibrium counterpart and originates from an imbalance between skyrmion creation and annihilation over a single field cycle, leading to a reversal of the period-averaged topological charge. We show that the re-entrant phase exists only in the dynamic response regime where the system can follow the drive, and is suppressed at higher driving frequencies. Our results establish periodic driving as a nonequilibrium control parameter for stabilizing and reversing skyrmion topology.

Magnetic skyrmions are topologically nontrivial, whirl-like spin textures that have emerged as promising information carriers for spintronic applications owing to their nanoscale size and efficient current-driven dynamics [1, 2]. Beyond their technological relevance, these topological objects provide a fertile platform for exploring novel physical phenomena including robust stabilities protected against external perturbations [3]. Originally proposed on theoretical grounds [4], magnetic skyrmions were later observed in bulk noncentrosymmetric magnets [5–8] and in thin-film systems with broken interfacial inversion symmetry [9–11]. Depending on the underlying microscopic interactions, skyrmions may originate from distinct mechanisms, including Dzyaloshinskii–Moriya interactions (DMIs) [12–14] and magnetic frustration [15–18].

In magnetic systems lacking inversion symmetry, spin–orbit coupling gives rise to an antisymmetric Dzyaloshinskii-Moriya type exchange interaction that favors chiral spin textures and stabilizes isolated skyrmions and skyrmion lattices through its competition with Heisenberg type exchange and Zeeman interactions. Hereby, skyrmions are characterized by a topological charge

$$\chi_Q = \frac{1}{4\pi}\int dx\, dy\, \mathbf{S}\cdot(\partial_x \mathbf{S}\times\partial_y \mathbf{S}) \tag{1}$$

which quantifies the topological nature of the spin configuration. In equilibrium, sufficiently strong magnetic fields destabilize skyrmions in favor of a uniformly polarized ferromagnetic state, thereby confining their stability to a finite field window between low-field magnetically ordered phases (e.g., helical or stripe-domain states) and the high-field ferromagnetic phase. However, this equilibrium picture can be profoundly modified by time-dependent magnetic fields, which open new pathways for topological transformations.

Dynamically driven nonequilibrium phase transitions arise in a wide variety of interacting many-particle systems subjected to oscillatory control parameters [19, 20]. A paradigmatic example is provided by dynamic phase transitions in ferromagnets driven by periodically oscillating magnetic fields [21, 22]. First observed in the kinetic Ising model [23], dynamic phase transitions manifest through qualitative changes in the magnetization when the field period is varied below the Curie temperature [24]. Subsequent studies have explored these transitions using mean-field approaches [25–31], Monte Carlo simulations [32–37], and experiments [38–45]. A remarkable outcome is the close correspondence between equilibrium and dynamic critical behavior, including identical universality classes revealed by finite-size scaling analyses [32, 46–54] and confirmed experimentally in ultrathin Co films [45]. Dynamical studies of magnetic skyrmions have mainly addressed the stability of individual skyrmions [55–57], whereas the collective nonequilibrium dynamics of extended skyrmion assemblies remain far less explored. Moreover, collective skyrmion dynamics can be induced by various external stimuli, such as applied fields [58, 59] or current injection [60–62]. While device-oriented studies naturally emphasize electrically driven mechanisms, time-dependent magnetic fields provide a general framework for probing collective dynamical phenomena.

In this Letter, we study the nonequilibrium dynamics of a two-dimensional magnet with DMIs under a periodically oscillating magnetic field. We consider a classical two-dimensional ferromagnetic Heisenberg model on a triangular lattice, described by the Hamiltonian

$$\begin{aligned}\mathcal{H} = &- J\sum_{\langle i,j\rangle}\mathbf{S}_i\cdot\mathbf{S}_j - \sum_{\langle i,j\rangle}\mathbf{D}_{ij}\cdot(\mathbf{S}_i\times\mathbf{S}_j)\\ &- A\sum_i (S_i^z)^2 - H(t)\sum_i S_i^z.\end{aligned} \tag{2}$$

Here $\mathbf{S}_i$ is a classical unit vector at lattice site i. The first term represents the nearest-neighbor Heisenberg-type ferromagnetic exchange interaction with coupling constant J. The second term describes the DMI, with

$$\mathbf{D}_{ij} = D\,\frac{\mathbf{r}_i - \mathbf{r}_j}{|\mathbf{r}_i - \mathbf{r}_j|} \times \hat{z}, \tag{3}$$

where $\mathbf{r}_i$ and $\mathbf{r}_j$ denote the real-space position vectors of spins at lattice sites i and j, respectively, and the interaction strength is fixed to $D = 1$ throughout this work. The third term denotes an easy-axis single-ion anisotropy along the out-of-plane (z) direction, with $A = 0.1$. The last term accounts for the coupling to an external magnetic field, $H(t)$, applied along the z axis, consisting of a static bias field h_b and a time-dependent component $h(t)$, chosen as a square wave with amplitude h_0 and half-period $t_{1/2}$. All sums $\langle i, j\rangle$ run over nearest-neighbor pairs. For simplicity, we set $k_{\mathrm{B}} = 1$ and $J = 1$ [63].

Monte Carlo simulations based on the single-spin Metropolis algorithm [64–67] were performed on triangular lattices of linear size $L = 120$ with periodic boundary conditions, as schematically illustrated in Fig. 1(a). Finite-size effects were assessed by additional simulations at larger system sizes, which produced essentially identical results. The system is gradually cooled from high temperatures, and after an initial thermalization stage at each temperature, simulations are carried out over 10^3 periods of the external field, during which thermal averages of physical observables are accumulated. Time is measured in units of one Monte Carlo step per site (MCSS).

In periodically driven spin systems, the period-averaged magnetization Q is commonly employed as a dynamical order parameter and is defined as [23]

$$Q = \frac{1}{P}\int_0^P M(t)\,dt, \tag{4}$$

where $M(t)$ is the instantaneous magnetization per spin, obtained from the sum of the out-of-plane spin components S_i^z, and $P = 2t_{1/2}$ denotes the period of the oscillating field. To characterize the topology, we compute the skyrmion number (topological charge) χ_Q, defined in Eq. (1). In the simulations, χ_Q is evaluated using a lattice discretization on elementary triangles (see the detailed discussion in [68]). Under a time-dependent magnetic field, $\chi_Q(t)$ becomes a time-dependent quantity. We therefore introduce the period-averaged skyrmion number,

$$\langle \chi_Q \rangle = \frac{1}{P}\int_0^P \chi_Q(t)\,dt, \tag{5}$$

which serves as a dynamical observable of the topological response of the system. Throughout this work, $\langle \chi_Q \rangle$ is reported per 10^2 unit cells.

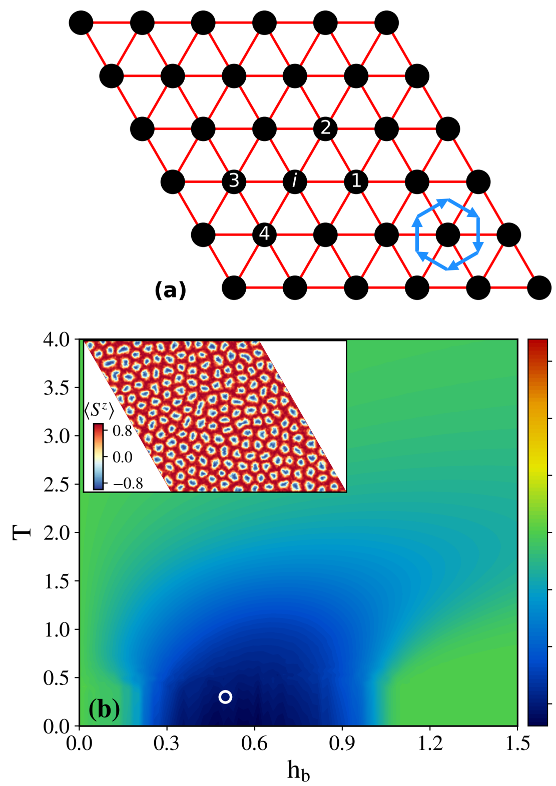

FIG. 1. (a) Schematic illustration of the triangular lattice geometry used in this work. Blue arrows indicate the DMI vectors $\mathbf{D}_{ij}$ between nearest-neighbor spins for positive D. (b) Equilibrium skyrmion number as a function of the magnetic field h_b and temperature T. The inset shows representative real-space spin textures at the white point marked in the phase diagram. The color scale denotes the out-of-plane spin component S^z.

The equilibrium topological response, quantified by the skyrmion number χ_Q, in the (h_b, T) plane is shown in Fig. 1(b). A blue region with negative χ_Q, corresponding to stabilized skyrmions, appears at intermediate bias fields and low-to-moderate temperatures due to the competition between Heisenberg exchange, DMIs, easy-axis anisotropy, and Zeeman energy. The inset displays a representative real-space spin texture from this region, specifically the one at the phase space point identified by the white circle in Fig. 1(b), forming a dense skyrmion lattice consistent with the negative topological charge. At low bias fields, χ_Q is negligible and stripe-domain configurations dominate. With increasing h_b, skyrmions emerge over a finite field window, beyond which the system crosses over to a uniformly polarized ferromagnetic phase with $\chi_Q \simeq 0$. As the temperature rises, the skyrmion-stabilized region shrinks and eventually vanishes, as thermal fluctuations destroy the topological order and drive the system into a paramagnetic state. A similar behavior has also been reported in realistic material-based models [12].

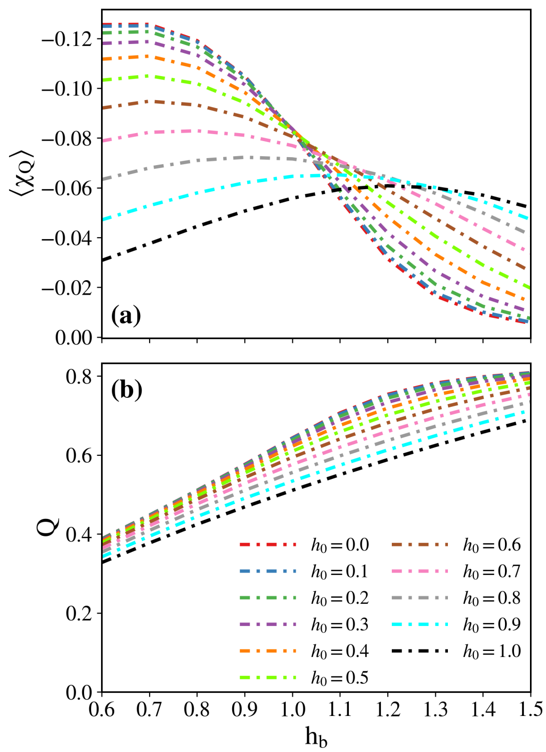

FIG. 2. (a) Period-averaged skyrmion number $\langle\chi_Q\rangle$ and (b) period-averaged magnetization Q as a function of the bias field h_b for several values of the oscillating field amplitude h_0, calculated for a half-period $t_{1/2} = 100$ MCSS.

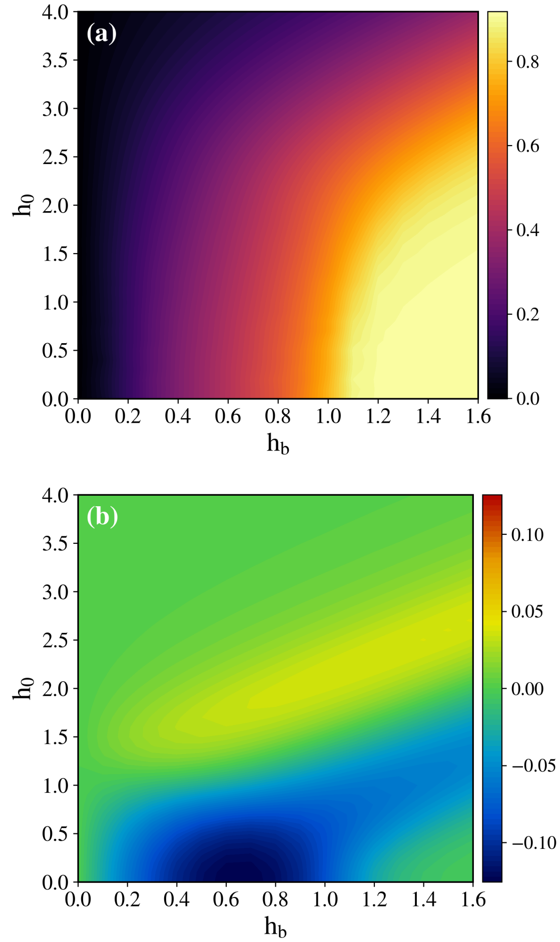

FIG. 3. (a) Period-averaged magnetization Q and (b) period-averaged skyrmion number $\langle\chi_Q\rangle$ in the (h_b, h_0) plane, computed at $t_{1/2} = 100$ MCSS. The color scale indicates the magnitude of the corresponding quantity in each panel.

Motivated by the equilibrium behavior in Fig. 1(b), we next investigate the nonequilibrium response of the system under a time-dependent magnetic field $h(t)$. Unless stated otherwise, results are shown at $T = 1$, a representative point within the equilibrium skyrmion-stabilized region. Figure 2(a) displays the period-averaged skyrmion number $\langle\chi_Q\rangle$ as a function of the bias field h_b for different oscillating-field amplitudes at half-period $t_{1/2} = 100$ MCSS, corresponding to a dynamic response regime in which the system can accommodate the driving field. The h_b range is chosen based on the equilibrium phase diagram to span the crossover from the skyrmion-stabilized phase to the polarized ferromagnetic phase. In the absence of an oscillating field ($h_0 = 0$), $\langle\chi_Q\rangle$ decreases smoothly with increasing h_b, consistent with the equilibrium crossover to the polarized phase with vanishing $\langle\chi_Q\rangle$. Introducing a time-dependent field suppresses the period-averaged skyrmion number within the skyrmion-stabilized regime by reducing the stability of skyrmion textures through the time dependence of the Zeeman term. For small h_0, $\langle\chi_Q\rangle$ retains a bias-field dependence similar to the static case, while for larger h_0, the transition broadens very relevantly.

To compare the evolution of topological order with conventional magnetic order, we analyze the period-averaged magnetization Q. As shown in Fig. 2(b), Q increases monotonically with h_b for all h_0, while the approach to saturation slows progressively with increasing oscillating-field amplitude. At low bias fields, Q remains small due to the DMI, which favors noncollinear spin textures and suppresses ferromagnetic alignment.

The bias-field dependence of the period-averaged skyrmion number already indicates that the topological response varies significantly with the oscillation amplitude. To obtain a global perspective, we explore the full (h_b, h_0) parameter space. Figure 3 presents the period-averaged magnetization and skyrmion number for a half-period $t_{1/2} = 100$ MCSS. As shown in Fig. 3(a), Q increases monotonically with h_b for all oscillation amplitudes h_0, consistent with the behavior observed in Fig. 2(b). Increasing h_b drives the system toward a polarized state, while the oscillating magnetic field shifts the onset of saturation to higher bias fields without changing

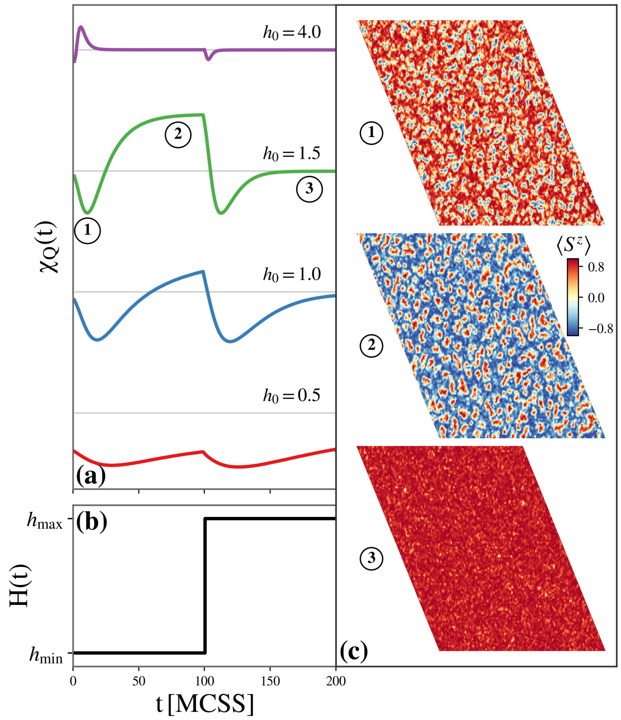

FIG. 4. Time evolution of: (a) the skyrmion number $\chi_Q(t)$ for several values of h_0 with $h_b = 0.7$, and (b) the total magnetic field over one cycle of the oscillating field. (c) Real-space spin textures corresponding to the circled points 1, 2, and 3 in panel (a) for $h_0 = 1.5$. The color scale denotes the out-of-plane spin component S^z. The half-period is fixed at $t_{1/2} = 100$ MCSS.

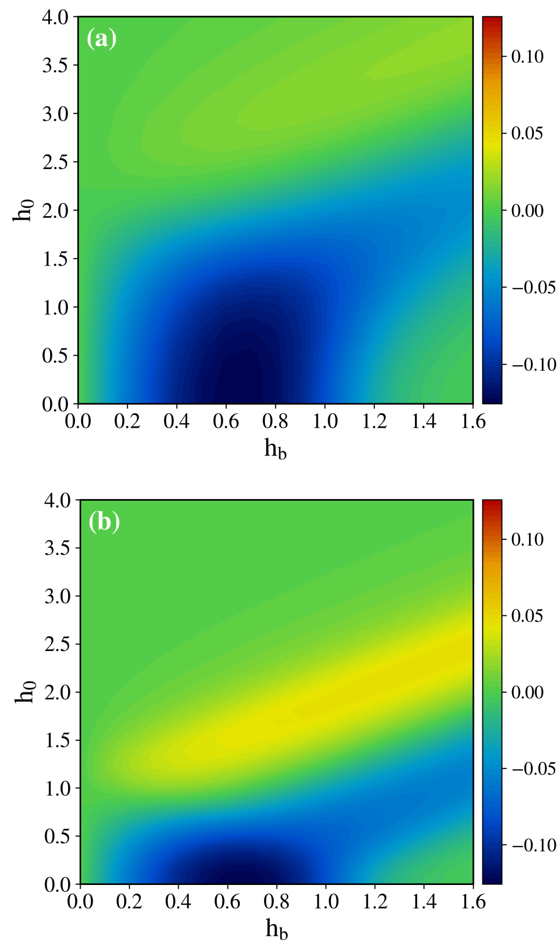

FIG. 5. Period-averaged skyrmion number $\langle \chi_Q \rangle$ in the (h_b, h_0) plane, computed over a half-period of (a) $t_{1/2} = 20$ MCSS, (b) $t_{1/2} = 200$ MCSS.

the overall monotonic trend. Although the conventional order parameter behaves as expected, by exhibiting a simple transition in between two equilibrium states that is being broadened and shifted by the oscillating magnetic field, the period-averaged skyrmion number, seen in Fig. 3(b), reveals a nontrivial nonequilibrium behavior in the (h_b, h_0) plane. For small field amplitudes ($h_0 \lesssim 1$), a negative region (blue) appears between the stripe-domain and polarized phases, so that this region closely resembles the equilibrium behavior of Fig. 1(b), indicating that weak oscillations minimally perturb the system. At intermediate amplitudes and bias fields $h_b \gtrsim 0.4$, however, $\langle \chi_Q \rangle$ re-emerges with the opposite topological sign, forming the yellow region in the phase diagram. This suggests that the skyrmion number behavior does not resemble the simple transition from one limiting behavior to the opposite, shown by Q, but instead displays the occurrence of a non-trivial intermediate state. The observed re-emergence of $\langle \chi_Q \rangle$ with opposite sign defines a dynamically re-entrant topological response, in which skyrmions undergo an imbalanced creation and annihilation over a full oscillation cycle, yielding a finite period-averaged topological charge with reversed sign. For sufficiently large h_0 and h_b, the re-entrant response disappears and $\langle \chi_Q \rangle \simeq 0$ across the entire bias-field range, and the system evolves into a dynamically polarized state.

The physics of the dynamically re-entrant phase in the dynamic response regime can be understood from the time evolution of the skyrmion number. Figure 4(a) depicts $\chi_Q(t)$ over a single field period for different amplitudes h_0 at fixed bias $h_b = 0.7$. The total magnetic field $H(t)$ is illustrated in Fig. 4(b). For small amplitudes ($h_0 = 0.5$), $\chi_Q(t)$ exhibits only a weak time dependence and remains negative. Increasing h_0 induces pronounced oscillations and sign changes in $\chi_Q(t)$, indicating that the external field drives the system between distinct topological states. This is particularly evident for $h_0 = 1.0$ and 1.5, where significant numbers of skyrmions are dynamically created and annihilated during the field cycle. For $h_0 = 1.5$, corresponding to the yellow region of positive period-averaged skyrmion numbers in Fig. 3(b), the positive contribution to χ_Q that is generated during the first half-period exceeds the negative contribution from the second half-period. This asymmetry in the topological response between successive half-periods arises from the superposition of the oscillatory and bias fields: during the first half-period, the negative oscillatory field dominates over the positive bias field, favoring formation of positive skyrmions, while in the second half-period the fields align driving the system toward a ferromagnetic state. The representative real-space spin textures in Fig. 4(c) support this scenario. Spin configurations sampled during the first and second half-periods exhibit positive and negative skyrmions, respectively, followed by a nearly polarized configuration toward the end of the cycle. This interplay between the bias field and the oscillatory drive also explains the inclined, ellipsoidal shape of the dynamically re-entrant skyrmion region, whose slope is approximately unity, indicating that the response is strongest along lines of nearly constant $h_0 - h_b$. Upon further increasing the field amplitude (e.g., $h_0 = 4.0$), the system evolves into a dynamically polarized state, with only small transient deviations in $\chi_Q(t)$ occurring near the field reversals.

Finally, we examine the effect of the field period, yet another control parameter of the oscillating magnetic field. Figure 5 displays the period-averaged skyrmion number $\langle \chi_Q \rangle$ in the (h_b, h_0) plane for different values of the half-period $t_{1/2}$. In the dynamic response regime, corresponding to long half-periods ($t_{1/2} = 100$ and 200 MCSS; the former already shown in Fig. 3(b)), a dynamically re-entrant region with positive topological charge (yellow) is clearly observed and becomes more pronounced as $t_{1/2}$ increases. This indicates that the system can respond effectively to the external field during each half-cycle. For shorter periods ($t_{1/2} = 20$ MCSS), shown in Fig. 5(a), the re-entrant region is strongly suppressed. In this fast-driving regime, the spins cannot follow the rapid field reversals, weakening the asymmetric creation and annihilation of skyrmions within a single cycle. Consistent with this picture, time-series analysis of the skyrmion number at $t_{1/2} = 20$ MCSS (see Fig. S1 in [68]) shows that the skyrmion dynamics exhibits a reduced ability to follow the oscillating magnetic field relative to the longer half-periods. We note that the dynamically re-entrant skyrmion response also persists at lower temperatures; see Fig. S2 in [68].

In summary, we have investigated the nonequilibrium dynamics of magnetic skyrmions in a two-dimensional ferromagnet driven by periodically oscillating magnetic fields using large-scale Monte Carlo simulations. By analyzing the period-averaged skyrmion number, we identify a dynamically re-entrant topological response in the (h_b, h_0) parameter space that has no equilibrium counterpart. This response, characterized by the suppression and subsequent reemergence of skyrmion order with reversed topological charge, is governed by the field amplitude h_0 and exists only in the dynamic response regime, disappearing at higher driving frequencies. Our results highlight the richness of nonequilibrium topological phenomena induced by time-dependent fields and establish oscillating magnetic fields as a powerful control parameter for the creation, annihilation, and topological reversal of skyrmion lattice states.

The numerical calculations reported in this paper were performed at TÜBİTAK ULAKBIM (Turkish agency), High Performance and Grid Computing Center (TRUBA Resources). The work of A.V. and N.G.F. was supported by the Engineering and Physical Sciences Research Council (grant EP/X026116/1 is acknowledged). Work at nanoGUNE was supported by the Spanish Ministry of Science and Innovation under the Maria de Maeztu Units of Excellence Program (Grant No. CEX2020-001038-M) and Project No. PID2024-155776NB-I00 (ULTRAMAN).

* zeynep.demir@deu.edu.tr
† erol.vatansever@deu.edu.tr
‡ alex.vasilopoulos@essex.ac.uk
§ nikolaos.fytas@essex.ac.uk
¶ a.berger@nanogune.eu

[1] N. Nagaosa and Y. Tokura, Nat. Nanotechnol. **8**, 899 (2013).
[2] B. Göbel, I. Mertig, and O. A. Tretiakov, Phys. Rep. **895**, 1 (2021).
[3] A. Fert, V. Cros, and J. Sampaio, Nat. Nanotechnol. **8**, 152 (2013).
[4] U. K. Rößler, A. N. Bogdanov, and C. Pfleiderer, Nature **442**, 797 (2006).
[5] S. Mühlbauer, B. Binz, F. Jonietz, C. Pfleiderer, A. Rosch, A. Neubauer, R. Georgii, and P. Böni, Science **323**, 915 (2009).
[6] X. Yu, Y. Onose, N. Kanazawa, J. Park, J. Han, Y. Matsui, N. Nagaosa, and Y. Tokura, Nature **465**, 901 (2010).
[7] W. Münzer, A. Neubauer, T. Adams, S. Mühlbauer, C. Franz, F. Jonietz, R. Georgii, P. Böni, B. Pedersen, M. Schmidt, A. Rosch, and C. Pfleiderer, Phys. Rev. B **81**, 041203(R) (2010).
[8] X. Z. Yu, N. Kanazawa, Y. Onose, K. Kimoto, W. Z. Zhang, S. Ishiwata, Y. Matsui, and Y. Tokura, Nat. Mater. **10**, 106 (2011).
[9] C. Moreau-Luchaire, C. Moutafis, N. Reyren, J. Sampaio, C. A. F. Vaz, N. Van Horne, K. Bouzehouane, K. Garcia, C. Deranlot, P. Warnicke, P. Wohlhüter, J.-M. George, M. Weigand, J. Raabe, V. Cros, and A. Fert, Nat. Nanotechnol. **11**, 444 (2016).
[10] A. Soumyanarayanan, M. Raju, A. L. Gonzalez Oyarce, A. K. C. Tan, M.-Y. Im, A. P. Petrović, P. Ho, K. H. Khoo, M. Tran, C. K. Gan, F. Ernult, and C. Panagopoulos, Nat. Mater. **16**, 898 (2017).
[11] W. Legrand, D. Maccariello, F. Ajejas, S. Collin, A. Vecchiola, K. Bouzehouane, N. Reyren, V. Cros, and A. Fert, Nat. Mater. **19**, 34 (2020).
[12] J. Liang, W. Wang, H. Du, A. Hallal, K. Garcia, M. Chshiev, A. Fert, and H. Yang, Phys. Rev. B **101**, 184401 (2020).
[13] J. Yuan, Y. Yang, Y. Cai, Y. Wu, Y. Chen, X. Yan, and

L. Shen, Phys. Rev. B **101**, 094420 (2020).
[14] E. Iroulart, F. A. Gómez Albarracín, and H. D. Rosales, Phys. Rev. B **110**, 155152 (2024).
[15] T. Okubo, S. Chung, and H. Kawamura, Phys. Rev. Lett. **108**, 017206 (2012).
[16] A. O. Leonov and M. Mostovoy, Nat. Commun. **6**, 8275 (2015).
[17] S. Hayami, S.-Z. Lin, and C. D. Batista, Phys. Rev. B **93**, 184413 (2016).
[18] D. Amoroso, P. Barone, and S. Picozzi, Nat. Commun. **11**, 5784 (2020).
[19] M. Henkel, H. Hinrichsen and S. Lübeck, *Non-Equilibrium Phase Transitions: Volume 1: Absorbing Phase Transitions* (Springer, USA, 2008).
[20] M. Rao, H.R. Krishnamurthy, and R. Pandit, Phys. Rev. B **42**, 856 (1990).
[21] B.K. Chakrabarti and M. Acharyya, Rev. Mod. Phys. **71**, 847 (1999).
[22] Y. Yüksel and E. Vatansever, J. Phys. D: Appl. Phys. **55**, 073002 (2022).
[23] T. Tomé and M.J. de Oliveira, Phys. Rev. A **41**, 4251 (1990).
[24] P. Riego, P. Vavassori, and A. Berger, Physica B **549**, 13 (2018).
[25] M.F. Zimmer, Phys. Rev. E **47**, 3950 (1993).
[26] G.M. Buendía and E. Machado, Phys. Rev. E **58**, 1260 (1998).
[27] H. Jang, M.J. Grimson, and C.K. Hall, Phys. Rev. E **68**, 046115 (2003).
[28] X. Shi, G. Wei, and L. Li, Phys. Lett. A **372**, 5922 (2008).
[29] A. Punya, R. Yimnirun, P. Laoratanakul, and Y. Laosiritaworn, Physica B **405**, 3482 (2010).
[30] R.A. Gallardo, O. Idigoras, P. Landeros and A. Berger, Phys. Rev. E **86**, 051101 (2012).
[31] P. Riego and A. Berger, Phys. Rev. E **91**, 062141 (2015).
[32] G. Korniss, C.J. White, P.A. Rikvold, and M.A. Novotny, Phys. Rev. E **63**, 016120 (2000).
[33] W.S. Lo and R.A. Pelcovits, Phys. Rev. A **42**, 7471 (1990).
[34] M. Acharyya and B.K. Chakrabarti, Phys. Rev. B **52**, 6550 (1995).
[35] M. Acharyya, Phys. Rev. E **56**, 1234 (1997).
[36] M. Acharyya, Phys. Rev. E **69**, 027105 (2004).
[37] G.M. Buendía and E. Machado, Phys. Rev. B **61**, 14686 (2000).
[38] Y.L. He and G. C. Wang, Phys. Rev. Lett. **70**, 2336 (1993).
[39] Q. Jiang, H.N. Yang, and G.C. Wang, Phys. Rev. B **52**, 14 911 (1995).
[40] J.-S. Suen and J.L. Erskine, Phys. Rev. Lett. **78**, 3567 (1997).
[41] W. Kleemann, J. Rhensius, O. Petracic, J. Ferre, J.P. Jamet, and H. Bernas, Phys. Rev. Lett. **99**, 097203 (2007).
[42] D.T. Robb, Y.H. Xu, O. Hellwig, J. McCord, A. Berger, M.A. Novotny, and P.A. Rikvold, Phys. Rev. B **78**, 134422 (2008).
[43] A. Berger, O. Idigoras, and P. Vavassori, Phys. Rev. Lett. **111**, 190602 (2013).
[44] P. Riego, P. Vavassori, and A. Berger, Phys. Rev. Lett. **118**, 117202 (2017).
[45] M. Quintana and A. Berger Phys. Rev. Lett. **131**, 116701 (2023).
[46] S.W. Sides, P.A. Rikvold, and M.A. Novotny, Phys. Rev. Lett. **81**, 834 (1998).
[47] S.W. Sides, P.A. Rikvold, and M.A. Novotny, Phys. Rev. E **59**, 2710 (1999).
[48] G.M. Buendía and P.A. Rikvold, Phys. Rev. E **78**, 051108 (2008).
[49] H. Park and M. Pleimling, Phys. Rev. E **87**, 032145 (2013).
[50] E. Vatansever, Physica A **511**, 232 (2018).
[51] E. Vatansever and N.G. Fytas, Phys. Rev. E **97**, 012122 (2018).
[52] E. Vatansever and N.G. Fytas, Phys. Rev. E **97**, 062146 (2018).
[53] A. Vasilopoulos, Z. Demir Vatansever, E. Vatansever, and N.G. Fytas, Phys. Rev. E **104**, 024108 (2021).
[54] Z. Demir Vatansever, Phys. Rev. E **106**, 054143 (2022).
[55] J. Hagemeister, N. Romming, K. von Bergmann, E. Y. Vedmedenko, and R. Wiesendanger, Nat. Commun. **6**, 8455 (2015).
[56] P. F. Bessarab, G. P. Müller, I. S. Lobanov, F. N. Rybakov, N. S. Kiselev, H. Jónsson, V. M. Uzdin, S. Blügel, L. Bergqvist, and A. Delin, Nat. Commun. **6**, 8455 (2015).
[57] L. Rózsa, E. Simon, K. Palotás, L. Udvardi, and L. Szunyogh, Phys. Rev. B **93**, 024417 (2016).
[58] S. L. Zhang, W. W. Wang, D. M. Burn, H. Peng, H. Berger, A. Bauer, C. Pfleiderer, G. van der Laan, and T. Hesjedal, Nat. Commun. **13**, 1593 (2022).
[59] B. Dai, D. Wu, S. A. Razavi, S. Xu, H. He, Q. Shu, M. Jackson, F. Mahfouzi, H. Huang, Q. Pan, Y. Cheng, T. Qu, T. Wang, L. Tai, K. Wong, N. Kioussis, and K. L. Wang, Sci. Adv. **9**, eade6836 (2023).
[60] X. Z. Yu, N. Kanazawa, W. Z. Zhang, T. Nagao, T. Hara, K. Kimoto, Y. Matsui, Y. Onose, and Y. Tokura, Nat. Commun. **3**, 988 (2012).
[61] J. Sampaio, V. Cros, S. Rohart, A. Thiaville, and A. Fert, Nat. Nanotechnol. **8**, 839 (2013).
[62] S. Woo, K. Litzius, B. Krüger, M.-Y. Im, L. Caretta, K. Richter, M. Mann, A. Krone, R. M. Reeve, M. Weigand, P. Agrawal, I. Lemesh, M.-A. Mawass, P. Fischer, M. Kläui, and G. S. D. Beach, Nat. Mater. **15**, 501 (2016).
[63] Here $k_B = 1$ is a choice of units, and fixing $J = 1$ sets the exchange Dzyaloshinskii-Moriya interaction energy scale.
[64] D.P. Landau and K. Binder, *A Guide to Monte Carlo Simulations in Statistical Physics* (Cambridge University Press, Cambridge, U.K., 2014).
[65] M.E.J. Newman and G.T. Barkema, *Monte Carlo Methods in Statistical Physics* (Oxford University Press, New York, 1999).
[66] K. Binder and D. W. Heermann, *Monte Carlo Simulation in Statistical Physics* (Springer, Verlag, 2010).
[67] N. Metropolis, A.W. Rosenbluth, M.N. Rosenbluth, A.H. Teller, and E. Teller, J. Chem. Phys. **21**, 1087 (1953).
[68] Supplementary information (2026), [URL will be inserted by publisher].